

# Accelerator Physics

The Taiwan Light Source (TLS) is the first large accelerator project in Taiwan. The goal was to build a high performance accelerator which provides a powerful and versatile light source to the users. Efforts were made to understand accelerator physics issues such as the linear lattice design, the orbit correction scheme, linear lattice optics correction and coupling correction methods, the non-linear beam dynamics effects in the presence of insertion devices and nonlinear fields, the transverse and longitudinal beam instabilities and cures, and the beam current lifetime related mechanisms, etc. As a result, we have reached or surpassed the design goal in terms of beam quality specifications. In this article, we summarize studies on some accelerator physics issues which constitute the major beam dynamics activities over the past years.

## Commissioning of Accelerators

Currently the facility is composed of a 50 MeV electron linac, a 10 Hz, 1.5 GeV (upgraded in 2000) booster synchrotron and a 1.5 GeV (upgraded in 1996) low emittance storage ring. The lattice structure of the booster is a FODO type. The storage ring is a combined-function, triple-bend-achromat (TBA) type with 6-fold symmetry and a circumference of 120 m. There are six long straight sections, each 6 m long, for the accommodation of injection elements, RF cavities, undulators, and wigglers.

The injector comprising of linac and 1.3 GeV booster synchrotron was successfully commissioned in July 1992. On February 23, 1993, beam circulation around the storage ring was accomplished. Beam was captured by the RF on April 13, 1993. Soon after beam was stored, the closed orbit distortions were corrected and some machine parameters were measured and compared with the theoretical values. The stored beam exceeded the design current of 200 mA in August 1993. In the

last decade, the accelerator performance has been continuously improved.

## Lattice and Emittance Coupling

Based on a number of design criteria, such as design energy, emittance, ring size, lifetime requirement, etc, we selected a 6-fold TBA lattice rather than the FODO or the Chasman-Green structures. Figure 1 shows the lattice functions of one cell. The nominal, or designed natural horizontal emittance of this lattice is 25.6 nm-rad at 1.5 GeV. The typical design beam size at one bending port is about 120  $\mu\text{m}$  and 60  $\mu\text{m}$  in the horizontal and vertical plane, respectively, and the photon brightness could be up in the range of  $10^{17}$  photon/s/mm<sup>2</sup>/mrad<sup>2</sup>/0.1%  $\Delta\lambda/\lambda$  with insertion devices. The photon spectrum could cover energy range from IR to soft x-ray. The horizontal dispersion functions are matched to be zero in the long straight sections in this nominal lattice. By varying the matching quadrupoles in the achromats, one can vary the natural emittance from 14 nm-rad to 57 nm-rad.

The existence of field errors and the accommodation of insertion devices affect the beam dynamics behavior and full investigation has been necessary. As a consequence, the specifications of the

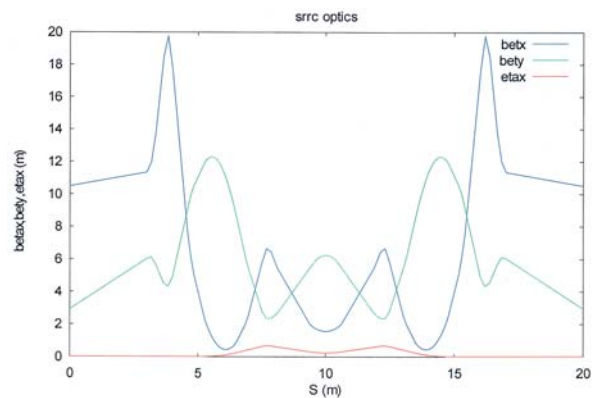


Fig. 1: Lattice functions of the NSRRC storage ring in one cell, six identical cells in bare lattice.

field errors of these beam line elements are obtained. It is found that, with the technically achievable magnetic field error tolerances, the dynamic aperture, i.e., the maximum allowable transverse amplitude of the survival particles, is slightly reduced from 35mm (H), 18 mm (V) for a pure bare lattice to 25 mm (H), 15 mm (V) at the center point of the injection section which is more than 50 times the beam size. In the presence of the insertion devices, the dynamic aperture is further reduced but still an acceptable level is obtained.

The machine working point is a very critical parameter in terms of the dynamic aperture. The selection of the working point near (7.30, 4.16) is based on the lattice matching condition, the optimization of the injection efficiency, the optimal dynamic aperture and emittance coupling, and the tune shift space for insertion devices, etc. The working point in the routine operations differs slightly from the design value in order to inject beam more efficiently and to optimize the coupling ratio, etc.

Gradient errors in the lattice elements can be due to the construction errors and power supply errors in quadrupole magnets as well as the feed-down from the off-center sextupole magnets. These gradient errors perturb the linear optics (betatron and dispersion functions). In the real machine, the equation of motion for the electron beam is coupled in the transverse planes. Therefore, the coupling elements such as skew quadrupoles, quadrupole magnet rolls, off-center sextupoles, can generate the betatron coupling or spurious vertical dispersion function. These perturbations can affect the dynamic aperture, injec-

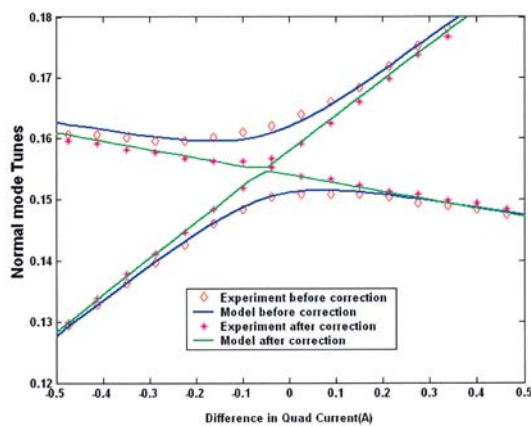


Fig. 2: Measured and model normal mode tunes of the NSRRC before and after correction.

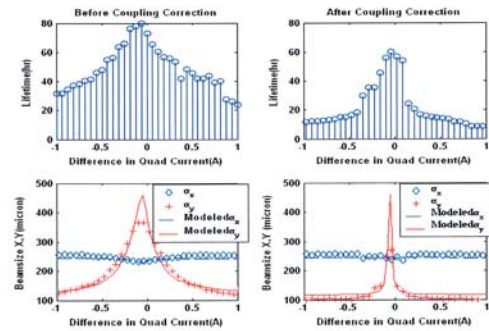


Fig. 3: Measured and model beam size as well as lifetime as a function of the quadrupole Q2 strength.

tion efficiency, vertical beam size, beam lifetime, and photon brightness. It is of primary importance to study and correct these errors in order to keep the machine performance as requested.

Applying two sophisticated programs called the "Linear Optics from Closed Orbit, LOCO" and "Cross Orbit Response Method", we are able to characterize the machine optics, coupling strength, corrector gains, corrector couplings, BPM gains, and BPM couplings, etc., and the linear optics and coupling errors can be corrected. It is also found that the major quadrupoles and coupling errors are from the off-center sextupoles. With the obtained errors, we can establish a virtual machine and compare it with the real machine in terms of the measurable parameters such as normal mode tunes, vertical dispersion, and coupling ratio, etc.

It is shown that the coupling strength  $|G_{1,-1,3}|$  can be corrected from 0.0119 to 0.0016. The normal mode tune, beam size at one dipole port and associated lifetime at 100 mA (no RF voltage modulation), and coupling strength, before and

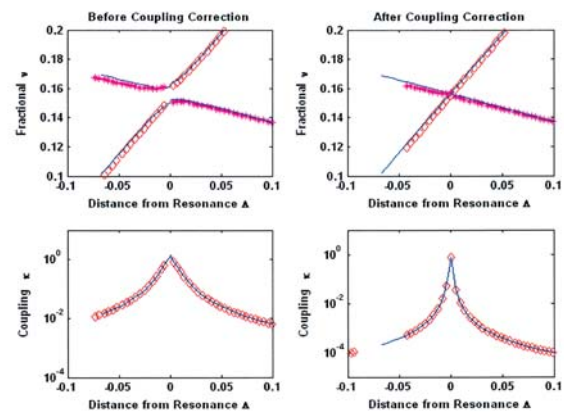


Fig. 4: Extracted coupling ratio as a function of tune difference away from the linear coupling resonance point for the NSRRC storage ring.

after correction, are shown in Figs. 2, 3, and 4.

### Lifetime

Beam lifetime is a very important issue in the light sources and usually more than ten hours is necessary at the initial stored beam current. Beam lifetime is primarily dominated by the Touschek scattering and gas scattering. Gas pressure needs to be lower than 1 nTorr and it requires careful handling of the vacuum components.

Touschek lifetime is approximately inversely proportional to the bunch density and proportional to the cubic of energy acceptance. By increasing the energy acceptance and reducing the bunch density, one can prolong the Touschek lifetime. Obviously, the transverse and longitudinal energy acceptance should be kept as high as possible. Dynamic aperture is a key issue in the transverse acceptance. Beam chamber size need to be large enough as well. Higher beam energy at 1.5 GeV helps increase the beam lifetime too.

Since the light source users demand a higher intensity of the synchrotron light and longer beam lifetime, one would like to reduce the bunch density in the longitudinal plane by using harmonic cavities or RF phase and magnitude modulations instead of using skew quads to increase the vertical beam size. In NSRRC, we apply an RF amplitude modulation at twice the synchrotron frequency to cure the longitudinal coupled-bunch instabilities and consequently, a higher beam lifetime is obtained. Up to now, we can easily get a beam lifetime of more than ten hours at 200 mA, in which the emittance coupling strength is about 1 %.

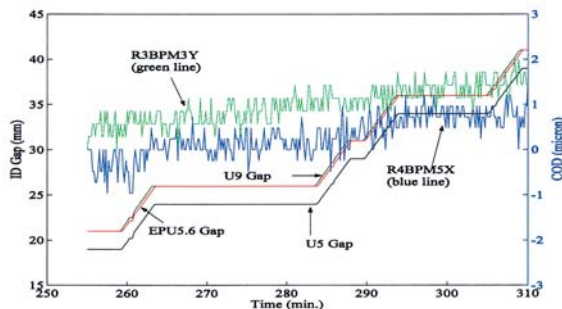


Fig. 5: With look-up tables and global orbit feedback system, the orbit drift during ID field scan is within a few micrometers.

### Orbit and Insertion Devices Operations

Closed orbit correction and orbit stability is of paramount importance in the operations of the light source too. In the design and construction phases, the magnetic field errors (1 ppm to 100 ppm) and alignment errors (about 150 micrometers rms) were well controlled and as a result the measured closed orbit distortions due to these errors are within tolerable range (a few mm) and also in good agreement with the model simulated results. Closed orbit distortions could be corrected down to several tens micrometers with various correction techniques.

Beam orbit is also very sensitive to mechanical vibrations, electronic and electricity noises, air and water thermal fluctuations, etc. Orbit stability should be kept within a few micrometers. Cares have been taken to reduce these sources. A global feedback system then corrects the residual orbit errors down to micrometer level.

One needs to study the beam dynamics effects in the presence of the insertion devices and the construction errors should be within the specifications in order to ensure minimum impact on the beam dynamics. Beam emittance could be changed from the nominal design value of 25.6 nm-rad to 21.5 nm-rad by adding 6 insertion devices in the long straight sections and it becomes 32.0 nm-rad if three more superconducting multipole wigglers are installed in the achromats. Simulations of the dynamic aperture with all 9 IDs have been carried out and the results show that, including all field errors in all magnets (measured or specified), the dynamic aperture reduces to an acceptable range of  $\pm 20$  mm (H) and  $\pm 10$  mm (V).

The orbit fluctuation could be more than 10 microns peak-to-peak if only the field compensation look-up tables are employed during ID field

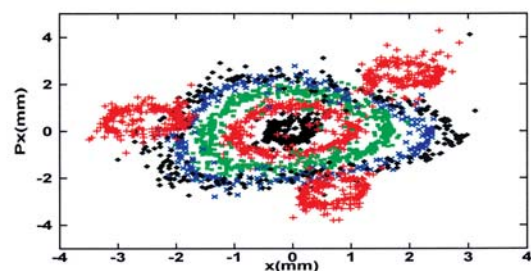


Fig. 6: Poincare map near 3<sup>rd</sup>-order resonance.

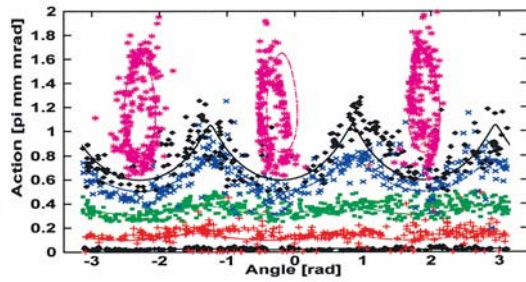


Fig. 7: Action-angle near 3<sup>rd</sup>-order resonance line.

scan. However, with the help of a fast digital orbit feedback system, the orbit variation can be maintained within a few micrometers (see Fig. 5).

### Nonlinear Beam Dynamics

Using phase space monitors consisting of turn-by-turn beam position detectors, transverse nonlinear beam dynamics studies were conducted in order to characterize the lattice parameters, such as the detuning factor, strengths of the nonlinear resonance driving sources. The resonance strengths around 3<sup>rd</sup>-order, 4<sup>th</sup>-order, as well as 5<sup>th</sup>-order nonlinear parametric resonances were measured. It is found that the resonance strengths, detuning parameters, etc., can be reproduced with a set of magnetic field errors. This set of field errors is consistent with the measured magnetic field errors. That means the inputs for dynamic aperture tracking are trustworthy. Figure 6 depicts the Poincaré phase-space map of the 3<sup>rd</sup>-order resonance and Fig. 7 is the corresponding action-angle plot.

Longitudinal beam dynamics behavior was investigated by applying both RF gap voltage amplitude and phase modulations. We studied these longitudinal beam dynamics with the Hamiltonian analysis method, particle tracking simulations, and measurement with a streak camera. In addition, the damping effects with uneven fills of the bunch trains were studied.

It was found that with the proper RF amplitude modulation at about twice the synchrotron frequency the re-distribution of the bunched beam into two or three beamlets are helpful to reduce the longitudinal instabilities and to increase beam current lifetime as well.

### Transverse Instabilities and Cures

The single bunch operation current could be more than 30 mA at 1.3 GeV when there were no

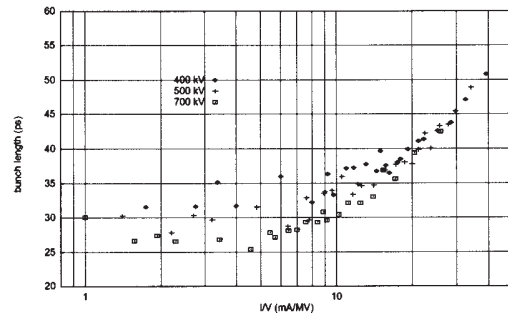


Fig. 8: Dependence of the bunch length as a function of bunch current and RF gap voltage. The microwave instability is clearly seen.

insertion devices in the beam line and the vertical vacuum chamber was 38 mm full size.

For the multi-bunch operation mode, we observed the beam oscillation in the vertical plane due to high gas pressure. The strength of the instability can be reduced by increasing the ring chromaticity (head-tail damping), increasing the ring energy to 1.5 GeV, improving the ring vacuum condition, leaving larger empty bucket train, and using a broadband transverse feedback damping system. The vertical instability can be suppressed to some extent with the help of the RF voltage modulation. For example, when the superconducting wavelength shifter is turned on, the local gas pressure increases by more than one order of magnitude and an RF modulation is applied to eliminate the vertical instability as mentioned above.

### Longitudinal Instabilities and Cures

By observing the bunch lengthening and the increase of energy spread as a function bunch current, we can study the longitudinal microwave instability. The microwave bunch lengthening for the short bunch is proportional to  $(IZ)^{1/(2+a)}$  in the Chao-Gareyte scaling law, where  $I$  is the bunch current,  $Z$  is the ring impedance, and  $a$  is the scaling factor. By fitting the observed bunch current at different RF gap voltages in Fig 8, we obtain the ring impedance of  $0.904 \Omega$  and  $a$  is 1.11. On the other hand, by employing the microwave instability model, we can fit the threshold current for different gap voltages and obtain the effective ring broadband impedance between  $0.86 \Omega$  and  $1.05 \Omega$ .

The longitudinal coupled-bunch instabilities (LCBI) are due to the higher-order modes (HOMs) of the conventional RF cavities, which cannot be fully suppressed with the damping antennae. We

observed that LCBI threshold current was as low as a few mA. This results in an increase of the beam energy oscillations and energy pulsing. One way to get rid of these instabilities is to remove the damping antennae inside the cavities and adjust the second tuner positions and cavity temperature as well. However, at NSRRC, this cannot reduce the instabilities to a satisfactory level.

Another cure for the LCBI is to use a bunch-by-bunch feedback system, which is currently under construction. The other way to cope with such instabilities is to apply an RF voltage modulation, in which the bunched beam is split into three beamlets so that the synchrotron tune is spread and Landau damping is invoked. This is the most effective operation mode for the NSRRC users run for the time being.

Moreover, we are constructing a HOM-free superconducting cavity to replace the existing conventional Doris cavities. The system is scheduled to be operational next year. The HOM-free cavity can eliminate the transverse and longitudinal coupled-bunch instabilities.

### Top-up Injection

Top-up injection scheme is an attractive operation mode as demonstrated by some light source machines, and NSRRC plans to adopt this operation mode in the near future. Major benefits with top-up mode are less thermal gradient in the accelerator components and photon beam line mirrors, more reduction of the insertion magnetic gap, and allowing smaller emittance lattice operations, etc. The lifetime issue is expected to be of less concern. We have demonstrated that the top-up injection

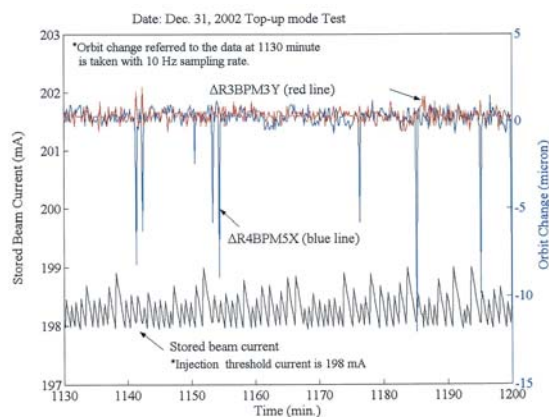


Fig. 9: Top-up mode test with SWLS.

is feasible with the magnetic field scan of insertion devices while keeping the orbit locked with the orbit feedback system, as shown in Fig. 9. Major concern of the top-up mode is the injection loss budget, i.e., the control of the radiation dosage level with the heavy-metal shutter open in the photon beam lines. Studies of the injector reliability, injection efficiency, and minimization of orbit perturbation during injection, etc., are ongoing.

### Author:

C. C. Kuo

National Synchrotron Radiation Research Center, Hsinchu, Taiwan

### Publications:

- C. C. Kuo, C. S. Hsue, J. C. Lee, M. H. Wang, and H. P. Chang, Proc. of PAC91, 2667 (1991).
- C. C. Kuo, J. Safranek, H. P. Chang, and K. T. Hsu, Proc. of PAC97, 843 (1997).
- C. C. Kuo, H. J. Tsai, H. P. Chang, M. H. Wang, G. H. Luo, K. T. Hsu, D. J. Wang, J. Safranek, and G. Portmann, Proc. of PAC03 (2003).
- C. C. Kuo, H. P. Chang, M. H. Wang, and W. T. Weng, Proc. of EPAC96, 697 (1996).
- C. C. Kuo, K. T. Hsu, H. P. Chang, C. Travier, G. J. Jan, and C. S. Hsue, Proc. of EPAC94, 1018 (1994).
- K. T. Hsu, C. C. Kuo, C. H. Kuo, H. P. Chang, Ch. Wang, H. J. Tsai, J. R. Chen, K. K. Lin, and R. C. Sah, Proc. of PAC99, 2409 (1999).
- H. P. Chang, C. H. Chang, J. Chen, K. T. Hsu, C. S. Hwang, C. C. Kuo, C. H. Kuo, and G. H. Luo, Proc. of PAC03 (2003).
- C. C. Kuo, H. P. Chang, J. Chen, K. T. Hsu, K. H. Hu, K. K. Lin, Y. C. Liu, H. J. Tsai, and T. S. Ueng, Proc. of PAC01, 1767 (2001).
- M.-H. Wang and S.Y. Lee, J. Appl. Phys. **92**, 555 (2002).

### Contact e-mail:

cckuo@nsrrc.org.tw